A computed tomography reconstruction algorithm based on multipurpose optimal criterion and simulated annealing theory

Hui Li (李 辉), Xiong Wan (万 雄), Taoli Liu (刘桃丽), Zhongshou Liu (刘仲寿), and Yanhua Zhu (朱彦华)

College of Automation, Nanchang University of Aeronautics, Nanchang 330063

Received September 24, 2006

Although emission spectral tomography (EST) combines emission spectral measurement with optical computed tomography (OCT), it is difficult to gain transient emission data from a large number of views, therefore, high precision OCT algorithms with few views ought to be studied for EST application. To improve the reconstruction precision in the case of few views, a new computed tomography reconstruction algorithm based on multipurpose optimal criterion and simulated annealing theory (multi-criterion simulated annealing reconstruction technique, MCSART) is proposed. This algorithm can suffice criterion of least squares, criterion of most uniformity, and criterion of most smoothness synchronously. We can get global optimal solution by MCSART algorithm with simulated annealing theory. The simulating experiment result shows that this algorithm is superior to the traditional algorithms under various noises.

OCIS codes: 110.6960, 100.3010, 300.6170.

Optical computed tomography (OCT) is an original testing technique based on laser measurement and computer information processing, which does not disturb the field distribution of the reconstructed object. OCT shows superiorities in testing thermo-physical parameters and diagnosing plasma[1−4], especially in physical parameters reconstruction of the three-dimensional (3D) fluid fields. Many methods are proposed for testing translucent object. These methods have different localizations in factual application, although they have got over the defect of disturbing the tested fields. Emission spectral tomography (EST) is widely used in recent years, which is combined emission spectral measurement with OCT[5]. The implement of EST system is becoming simple and effective with the development of photo-detectors such as charge coupled device (CCD). Generally, the EST system only can get data under few views and limited angle, which is named un-sufficient data. Traditional algorithms for un-sufficient data generally are iterative algorithms based on the series-expansion principle. They all have merit and restriction respectively[6−9]. To solve the problem of un-sufficient data of EST system, a new computed tomography reconstruction algorithm based on multipurpose optimal criterion and simulated annealing theory (MCSART) is proposed.

The problem of reconstruction of a source function can be formulated as the inversion of radon transform in terms of mathematical point. The two-dimensional (2D) reconstruction problem shown in Fig. 1 can be presented as

$$p(t,\phi)=\int_{-\infty}^{\infty} f(x,y)\mathrm{d}s, \tag{1}$$

where $p(t,\phi)$ are the projection data, which is integrated along the s axis, and $f(x,y)$ is the unknown source function. The Cartesian coordinate system (t,s) is rotated at an angle ϕ relative to the basic system (x,y).

MCSART algorithm needs the continuous image function to be divided at the beginning of the process. Therefore, we should divide the reconstruction area into J ($J=M\times N$) rectangular grids (Fig. 2), where M is the number of spaced points in the x direction, N in the y direction, and J is the total number of pixels which need to be reconstructed by the algorithm. Here M equals to N, the reconstruction of f at any point (x,y) is given by

$$f(x,y)=\sum_{j=1}^{J} f_j b(x-x_j,y-y_j), \tag{2}$$

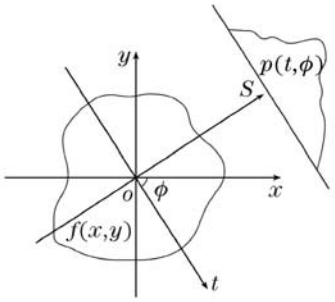

Fig. 1. Relationship between projection and source function.

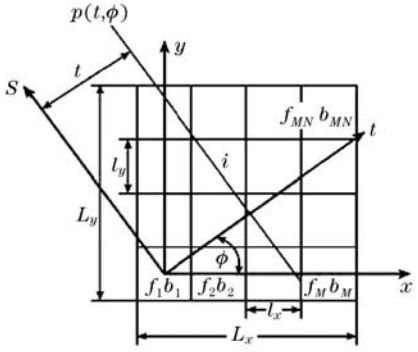

Fig. 2. Grid partition of series-expansion principle.

1671-7694/2007/060340-04

where f_j is the discrete image function value corresponding to the position (x_j, y_j), and b is the basis function. In this work, sinc basis function is used in the MCSART algorithm, since it can get high reconstruction precision in most case, which is expressed as

$$b_{xy} = \mathrm{sinc}[\frac{1}{l_x}(x - ml_x)]\mathrm{sinc}[\frac{1}{l_y}(y - nl_y)], \tag{3}$$

where l_x and l_y are the sampling periods of space in the x and y directions, respectively. Combining Eqs. (1)—(3), we obtain

$$p_i(t, \phi) = \sum_{j=1}^{J} f_j \int_i b(x - x_j, y - y_j)\mathrm{d}s = \sum_{j=1}^{J} w_{ij} f_j, \tag{4}$$

where i is the number of projective ray, and w_{ij} is the projection coefficient of the basis function

$$w_{ij} = \begin{cases} l_x|\sec\phi|\mathrm{sinc}\left(\frac{t\sec\phi + ml_x\tan\phi - nl_y}{l_y}\right), \\ \qquad 0 \le |\tan\phi| \le \frac{l_y}{l_x} \\ \frac{l_y|\sec\phi|}{|\tan\phi|}\mathrm{sinc}\left(\frac{t\sec\phi + ml_x\tan\phi - nl_y}{l_x\tan\phi}\right), \\ \qquad \frac{l_y}{l_x} < |\tan\phi| < \infty \\ l_y\mathrm{sinc}\left(\frac{t + ml_x}{l_x}\right), \qquad |\tan\phi| = \infty \end{cases} \tag{5}$$

The matrix form of Eq. (4) is

$$\mathbf{P} = \mathbf{WF}, \tag{6}$$

where $\mathbf{P}$ is the measurement vector, $\mathbf{W}$ is the projection matrix of the basis function, and $\mathbf{F}$ is the object vector. The dimension of $\mathbf{P}$ is $I = \mathrm{KV} \times \mathrm{RPV}$, where KV is the number of projection views, and RPV is the number of rays in each view. The dimension of $\mathbf{W}$ is $I \times J$, where J is the dimension of $\mathbf{F}$. In the practical application, Eq. (6) should be modified as

$$\mathbf{P} = \mathbf{WF} + \mathbf{E}, \tag{7}$$

where $\mathbf{E}$ is the error Vector. Then the problem of image reconstruction can be formulated as to calculate the estimated object vector ($\hat{\mathbf{F}}$) by the measurement vector and the projection matrix with given optimal criterion.

Construction of multi-criterion optimal function. Based on SIRT algorithm, MCSART algorithm suffices criterion of least squares, the corresponding aim function can be expressed as

$$\Phi_1(\hat{\mathbf{F}}) = (\mathbf{P} - \mathbf{W}\hat{\mathbf{F}})^{\mathrm{T}}(\mathbf{P} - \mathbf{W}\hat{\mathbf{F}}). \tag{8}$$

Equation (7) needs more restriction in terms of the relationship between each pixel. There are two facts needed to be considered in the actual image. 1) The values of the adjacent pixels are closely in the reconstruction image which expresses the parameter of the 3D fluid fields. Considering the above fact, we need another aim function

$$\Phi_2(\hat{\mathbf{F}}) = \sum_{j\in\zeta}(f_j - \frac{1}{8}\sum_{k\in\zeta_j} f_k)^2, \tag{9}$$

where ζ is the congregate of pixels which do not approach to the boundary of the image, ζ_j is the congregate of eight pixels which near the f_j. Generally, Eq. (9) takes the matrix form

$$\Phi_2(\hat{\mathbf{F}}) = \hat{\mathbf{F}}^T\mathbf{B}\hat{\mathbf{F}}, \tag{10}$$

$\mathbf{B}$ is defined as

$$\mathbf{B} = \sum_{j\in\zeta}\mathbf{S}_j\mathbf{S}_j^{\mathrm{T}}, \tag{11}$$

where $\mathbf{S}_j$ is the column vector. The unit of $\mathbf{S}_j$ is defined as

$$S_{jk} = \begin{cases} 1, & k = j \\ -\frac{1}{8}, & k \in E_j \\ -\frac{1}{8}, & k \in V_j \\ 0, & \text{others} \end{cases}, \tag{12}$$

where E_j and V_j are the congregations of pixels, which approach to the boundary and four angles of f_j, respectively.

2) The values of the pixels are changed slowly in the reconstruction image which expresses the parameter of the 3D fluid fields. We should ensure the square deviation of the pixel values as small as possible, then we obtain another aim function

$$\Phi_3(\hat{\mathbf{F}}) = \hat{\mathbf{F}}^T\hat{\mathbf{F}}. \tag{13}$$

Combining Eqs. (8), (10), and (13) according to multipurpose optimal theory, we obtain the final aim function

$$\Phi(\hat{\mathbf{F}}) = \tau_1(\mathbf{P} - \mathbf{W}\hat{\mathbf{F}})^{\mathrm{T}}(\mathbf{P} - \mathbf{W}\hat{\mathbf{F}}) + \tau_2\hat{\mathbf{F}}^{\mathrm{T}}\mathbf{B}\hat{\mathbf{F}} + \tau_3\hat{\mathbf{F}}^{\mathrm{T}}\hat{\mathbf{F}}, \tag{14}$$

where τ_1, τ_2, and τ_3 are the weight coefficients. We should set the weight coefficients according to the identity of the reconstructed image in the practical application. The weight coefficients are related as

$$\tau_1 + \tau_2 + \tau_3 = 1. \tag{15}$$

The basic method of simulated annealing theory is that we can simulate an optimal problem as a physical system. We get the global optimal solution to the optimal problem by simulating the annealing process. We adopt Eq. (14) as the optimizing function, where $\tau_1 = \tau_2 = \tau_3 = \frac{1}{3}$, then the steps of the MCSART algorithm are:

1) Selecting the original image, $\mathbf{F}^{(0)} = \mathbf{W}^{\mathrm{T}}\mathbf{P}$.

2) λ_k is the random selected by the computer according to the simulated annealing theory. λ_k is a positive number named relaxation parameter which obeys $N(\lambda_0, 1/\log(k+1))$ normal distribution, where k is the iteration times, λ_0 is the best relaxation parameter. λ_0 can be ascertained beforehand according to the reconstruction conditions.

3) The iterative format (the new solution generator) can be expressed as

$$\mathbf{F}^{(k+1)} = \mathbf{F}^{(k)} + \lambda_k\mathbf{W}^{\mathrm{T}}[\mathbf{P} - \mathbf{WF}^{(k)}], \tag{16}$$

where $\mathbf{F}^{(k)}$ is the image vector after k times iteration and $\mathbf{F}^{(k+1)}$ is that after $k+1$ times.

4) New solution accepting criterion. The function value of the aim function likes the energy of the annealing process. It indicates that the iteration goes to the optimal direction and λ_k is appropriate, if $\Phi[\mathbf{F}^{(k+1)}] \le \Phi[\mathbf{F}^{(k)}]$,

and the iteration will keep on, otherwise it indicates that the iteration goes to the worse direction. We may not get the global optimal solution but the local ones if we give up the result of this iteration. Therefore, we need to set the accept probability according to the simulated annealing theory. The method can be that R is a number random selected by the computer, which obeys the $N(0,1)$ normal distribution. If $|R| < 2/\log(k+1)$, the new solution is accepted, otherwise it is given up, and the algorithm goes to Step 2) to select a new reflection parameter.

5) Algorithm exiting criterion. The algorithm will exit if $\|\mathbf{F}^{(k+1)} - \mathbf{F}^{(k)}\| < \varepsilon$ (ε is a infinitesimal positive number, such as 10^{-6}), then $\mathbf{F}^{(k+1)}$ will be the final solution.

Asymmetrical four-peak Gaussian function was used in the numerical simulation (Fig. 3), which is expressed as

$$f(x,y) = \sum_{i=1}^{4} a_i \exp\left[-\frac{4\ln 2}{0.2^2}(x-x_i)^2 - \frac{4\ln 2}{0.2^2}(y-y_i)^2\right],$$

$$x_1 = 0.15,\ y_1 = 0.15;\ x_2 = 0.15,\ y_2 = -0.15;$$

$$x_3 = -0.15,\ y_3 = 0.15;\ x_4 = -0.15,\ y_4 = -0.15;$$

$$a_1 = 1,\ a_2 = 0.4,\ a_3 = 0.6,\ a_4 = 0.8. \tag{17}$$

We can obtain the projection p_i by numerical line integral with Simpson method. We add Gaussian noises to the projection to test the effect of measurement errors and noises. The projection added noises can be written as

$$p_i' = [1 + N(\mu, \sigma^2)]p_i, \tag{18}$$

where $\mu = 0$ is the mean of the noises, and σ^2 is the mean various.

Three error measures are defined. The first is the average absolute error

$$\alpha = \sum_{j=1}^{J} |f_j - \hat{f}_j| \Big/ (f_{\max} \times J), \tag{19}$$

the second is the maximum error

$$\beta = \left|f_j - \hat{f}_j\right|_{\max} \Big/ f_{\max}, \tag{20}$$

the third is the mean-square error

$$\gamma = \left(\sum_{j=1}^{J} (f_j - \hat{f}_j) \Big/ \sum_{j=1}^{J} f_j^2\right)^{\frac{1}{2}}, \tag{21}$$

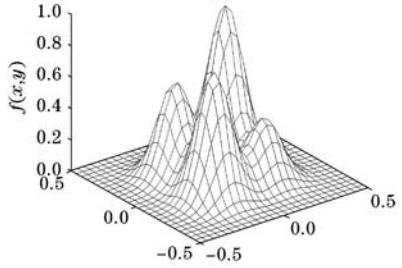

Fig. 3. Surface of asymmetrical four-peak Gaussian function.

where f_j is the true source that has the maximum value $f_{\max}$, and $\hat{f}_j$ is the reconstruction.

To test the reconstruction effect of the MCSART algorithm, we select ART algorithm and SIRT algorithm to compare with it. In this work, the reconstruction conditions are as follows:

·Projection views: four angels evenly spaced over a 180° total view (0°, 45°, 90°, and 135°).

·Sampling points in per projection view: RPV = 26, then the total number of the rays is $I = 4 \times 26 = 104$.

·Spatial resolving power of reconstruction area: $J = M \times N = 26 \times 26 = 676$.

·Iterative times (IT): IT = 50.

·Added noises: there are two case $\sigma^2 = 0$ and $\sigma^2 = 0.06$.

The reconstruction errors of three algorithms are shown in Table 1, the bold figures are the best reconstruction

Table 1. Reconstruction Errors α, β, γ

Algorithm	Noise (σ^2)	α (%)	β (%)	γ (%)
ART	0	1.23	10.57	9.15
	0.06	1.51	12.97	11.40
SIRT	0	0.77	6.46	6.06
	0.06	1.32	11.02	10.15
MCSART	0	0.70	5.52	5.33
	0.06	1.27	13.16	9.87

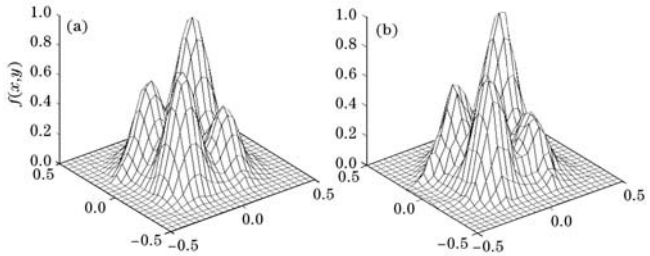

Fig. 4. Reconstruction image with MCSART algorithm. (a) $\sigma^2 = 0$; (b) $\sigma^2 = 0.06$.

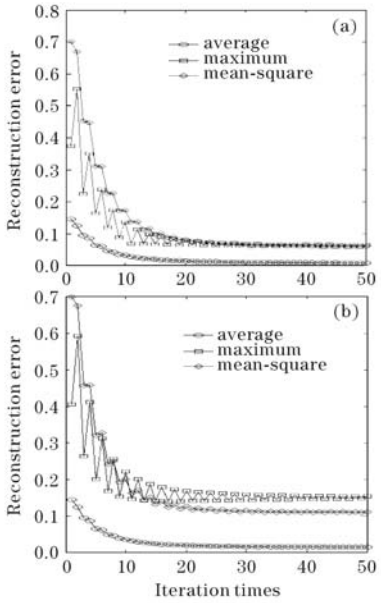

Fig. 5. Convergence of MCSART algorithm. (a) $\sigma^2 = 0$; (b) $\sigma^2 = 0.06$.

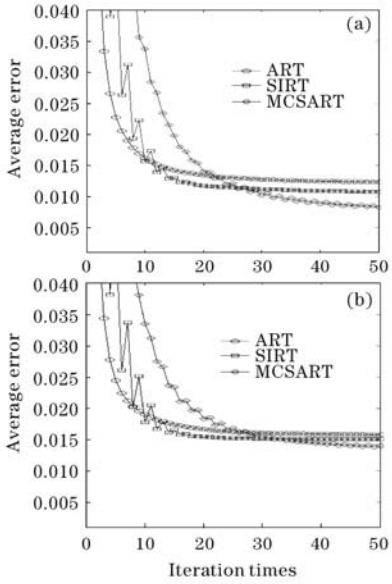

Fig. 6. Convergences of three algorithms. (a) $\sigma^2 = 0$; (b) $\sigma^2 = 0.06$.

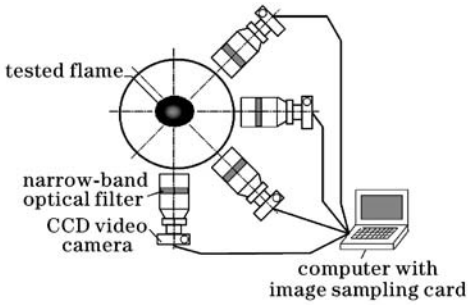

Fig. 7. EST system applied in the experiment.

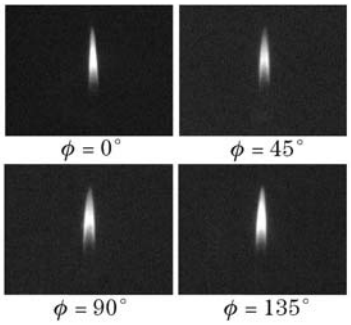

Fig. 8. Four BMP images for different view angles.

result of three algorithms under the same condition. The reconstruction results are shown in Figs. 4—6.

The emission coefficients field of a candle flame is reconstructed with the MCSART algorithm. The EST system is shown in Fig. 7, consisting of four narrow-band optical filters, four CCD video cameras, and a computer with a four-in-one image card. The image card can send the four-way real-time image data to the memory of the computer by PCI port. The four BMP images captured are shown in Fig. 8. The reconstructed relative intensity

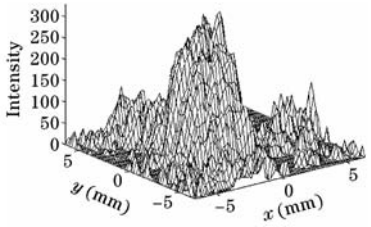

Fig. 9. One layer of the 3D reconstruction.

of emission coefficients field of the candle flame is shown in Fig. 9.

In conclusion, the reconstruction results of MCSART algorithm are better than others under the same conditions, except that maximum error is worse than that of SIRT under noising condition. The average error of MCSART algorithm reduces about 43% compared with that of ART algorithm when there is no noise. The reconstruction precision is improved greatly with the MCSART algorithm. The convergence of MCSART algorithm is better than others. And MCSART algorithm converges rapidly. The experiment indicates that the four-view computed tomography of EST system with MCSART algorithm can get good result. Therefore, there is great applied potential of MCSART algorithm in EST system under un-sufficient data conditions. The experiment of the emission spectral tomography with MCSART shows the feasibility of the algorithm in EST system.

This work was supported by the Chinese Natural Science Foundation of China (No. 60577016), the Foundation (No. 0512034) of Jiangxi Natural Science, the Science and Technology Program (No. 2006-164) of Jiangxi Provincial Department of Education, and the Program (No. 2005-314) of Key Laboratory of Nondestructive Testing Technology, Ministry of Education. H. Li's e-mail address is lihuiys@163.com.

References

1. X. Wan, Y. Gao, C. Wang, S. Le, and S. Yu, Opt. Eng. **42,** 2659 (2003).
2. X. Wan, S. Yu, Y. Gao, and Q. Zhu, Opt. Eng. **43,** 1244 (2004).
3. X. Wan, X. He, and Y. Gao, Acta Opt. Sin. (in Chinese) **23,** 1433 (2003).
4. X. Wan, Y. Gao, and X. He, Acta Opt. Sin. (in Chinese) **23,** 1099 (2003).
5. X. Wan, S. Yu, C. Wang, S. Le, B. Li, and X. He, Acta Phys. Sin. (in Chinese) **53,** 3104 (2004).
6. I. Braslavsky and S. G. Lipson, in *IMechE Transactions of Optical Methods and Data Processing in Heat and Fluid Flow* (1998) p.423.
7. A. Brunetti and B. Golosio, Med. Phys. **28,** 462 (2001).
8. B. Zhang, Y. Song, Y. Song, and A. He, Chin. J. Lasers (in Chinese) **33,** 531 (2006).
9. X. Wan, Y. Gao, and Y. Wang, Chin. Opt. Lett. **1,** 78 (2003).